Mitotic Centromere–associated Kinesin Is Important for Anaphase Chromosome Segregation

Todd Maney, Andrew W. Hunter, Mike Wagenbach, and Linda Wordeman

Department of Physiology and Biophysics, University of Washington School of Medicine, Seattle, Washington 98195

Abstract. Mitotic centromere–associated kinesin (MCAK) is recruited to the centromere at prophase and remains centromere associated until after telophase. MCAK is a homodimer that is encoded by a single gene and has no associated subunits. A motorless version of MCAK that binds centromeres but not microtubules disrupts chromosome segregation during anaphase. Antisense-induced depletion of MCAK results in the same defect. MCAK overexpression induces centromere-independent bundling and eventual loss of spindle microtubule polymer suggesting that centromere-associated bundling and/or depolymerization activity is required for anaphase. Live cell imaging indicates that MCAK may be required to coordinate the onset of sister centromere separation.

Key words: MCAK • centromere • kinesin • mitosis • anaphase

During mitosis the cell cytoplasm undergoes a comprehensive structural and biochemical transformation. Microtubules are reorganized to form a bipolar, interdigitating framework of fibers emanating from each of two migrating centrosomes (for review see Karsenti and Hyman, 1996). The mitotic spindle is a dynamic structure that exhibits several simultaneous microtubule behaviors such as dynamic instability (Mitchison et al., 1986; Wadsworth and Salmon, 1986) and microtubule flux (Mitchison, 1989; Sawin and Mitchison, 1991). Condensed chromosomes attach to this framework via a specialized structure on their surface known as the kinetochore. Upon attachment to the spindle microtubules, the previously inert chromosomes become integrated into the dynamic activity of the mitotic spindle (Skibbens et al., 1993; Rieder and Salmon, 1994; for review see Inou'e, 1997). Complete understanding of centromere function is complicated by the superimposition of a multitude of motor activities on top of dynamic microtubule behavior within an extremely short window of time.

Before and during nuclear envelope breakdown, three microtubule-dependent motors are targeted specifically to the centromere. The dynein/dynactin complex, which is also involved in spindle assembly (Merdes et al., 1996), may be involved in early minus-end–directed prometaphase chromosome movements (Echeverri et al., 1996) and also anaphase onset (Starr et al., 1998). The kinesin-related protein CENP-E has been implicated in both the establishment of bipolar connections and the alignment of chromosomes on the metaphase plate (Schaar et al., 1997; Wood et al., 1997). These are activities associated with later stages of prometaphase and metaphase. Interestingly, both dynein/dynactin and CENP-E appear to be released from the kinetochore during mitosis after these critical stages have been completed. Kinetochore-associated dynein/dynactin is undetectable after metaphase (Echeverri et al., 1996) and CENP-E is lost from the kinetochore after anaphase A (Yen et al., 1992; Brown et al., 1996). In contrast, the third centromere–associated microtubule motor, MCAK,[1] (mitotic centromere–associated kinesin) is detectable on mitotic centromeres through telophase (Wordeman and Mitchison, 1995). This persistent centromere association may be functionally significant for we report here that MCAK may be dispensable for prometaphase events. Rather, MCAK appears to be required for the onset of anaphase chromosome movement.

Genetic systems such as *Saccharomyces cerevisiae* have been instrumental in dissecting spindle and centromere function in vivo (for review see Hoyt and Geiser, 1996). However, the centromere of *S. cerevisiae* differs from that of mammalian spindles in many respects. Many orders of magnitude less DNA is present in the centromere of *S. cerevisiae* compared with other eukaryotic cells (Bloom, 1993). The centromere-associated proteins that bind to

Address all correspondence to Linda Wordeman, Department of Physiology and Biophysics, Box 357290, G424 Health Sciences, University of Washington School of Medicine, Seattle, WA 98195. Tel.: (206) 543-5135. Fax: (206) 685-0619. E-mail: worde@u.washington.edu

1. *Abbreviations used in this paper*: GFP, green fluorescent protein; MCAK, mitotic centromere–associated kinesin.

centromere DNA and have been implicated in organizing centromere structure in mammals are substantially different from analogous proteins in *S. cerevisiae* with the possible exception of CENP-C (Meluh and Koshland, 1995). The kinetochore in *S. cerevisiae* attaches to a single microtubule rather than the 10–50 microtubules that are attached to mammalian kinetochores (Brinkley and Cartwright, 1971; Winey et al., 1995; McEwen et al., 1997; for review see Bloom, 1993). This obviates the need for any mechanism for coordination between groups of microtubules imbedded in a single *S. cerevisiae* centromere. Significantly, in *S. cerevisiae* a metaphase plate is never established, despite the fact that prometaphase and anaphase chromosome motility is qualitatively similar in yeast and mammalian cells (Straight et al., 1997).

MCAK's localization relative to other kinetochore motors places it in a prime location for interacting with microtubule ends imbedded in the kinetochore (Wordeman and Mitchison, 1995). Immunodepletion of a putative *Xenopus* homologue of MCAK (XKCM1) disrupts mitotic spindle assembly and reduced the catastrophe frequency of microtubules in mitotic extracts suggesting that this motor may be able to promote microtubule depolymerization (Walczak et al., 1996). We report here that MCAK overexpression results in bundling and eventual loss of spindle microtubule polymer, whereas both MCAK depletion and a dominant-negative mutant of MCAK produces lagging chromosomes during anaphase chromosome segregation. Live cell imaging indicates that these lagging chromosomes result from delayed sister chromatid separation. We suggest that MCAK may be required to bundle and/or destabilize kinetochore microtubules, specifically at the metaphase-to-anaphase transition when kinetochore-associated microtubules have been observed to reach peak numbers (McEwen et al., 1997) and stability (Zhai et al., 1995). Because no MCAK-related motor has been identified in the *S. cerevisiae* genome, MCAK may be specifically required for organisms that establish a metaphase plate and that contain larger, multi-microtubular kinetochores.

Materials and Methods

Genomic Southerns and Immunoprecipitations

High molecular weight genomic DNA was isolated from logarithmically growing CHO-K1 cells as per Sambrook et al. (1989). DNA was digested overnight in BamHI, HindIII, or XbaI, run on a large agarose gel, and then blotted onto nylon membrane. Probes were synthesized from specific regions of MCAK using a random priming kit (Boehringer Mannheim Corp., Indianapolis, IN). Hybridizations were performed at 50–55°C overnight and exposed to Kodak X-Omat film.

Monolayer cultures of CHO-K1 cells were labeled overnight with 100 μCi [S^{35}]methionine-containing MEMα medium in 1/2 vol (5 ml) in a 100-cm^2 dish. Cells were removed with EDTA, washed, and then lysed in either radioimmunoprecipitation assay (RIPA) buffer (150 mM NaCl, 1.0% NP-40, 0.5% deoxycholate, 0.1% SDS, PMSF, 50 mM Tris, pH 7.5) or NP-40 buffer (150 mM NaCl, 1.0% NP-40, PMSF, 50 mM Tris, pH 8.0). 1 μl of affinity-purified rabbit anti-MCAK antisera or nonimmune rabbit IgG was added to the clarified lysate and incubated 1 h at 4°C with rotation. 50 μl protein A–coated beads (Repligen Corp., Needham, MA) were added to the lysate and incubated 1 h at 4°C. Beads were spun down, washed in PBS, and then resuspended in SDS-PAGE buffer. Samples were run on a 5–12% gradient gel (Novex, San Diego, CA), dried, and then exposed to Kodak X-Omat film.

BExp-MCAK Expression and Hydrodynamic Analysis

The MCAK coding region in pBluescript II (pMX403) was mutagenized to produce a COOH-terminal 6× histidine addition and a 5′ leader sequence containing NdeI and HpaI sites plus a bacterial ribosome binding site (pMX803). This MCAK gene sequence was cloned into BamHI to NotI sites of pVL1383 (PharMingen, San Diego, CA), a baculovirus transfer vector, to place MCAK under the control of the polyhedrin promoter (pMX1001). This construct and BaculoGold viral DNA (PharMingen) was used to prepare recombinant virus for infection of Sf9 cells. 3 d of expression resulted in maximum MCAK6His expression (BExp-MCAK). BExp-MCAK was purified on a NTA-agarose column (Qiagen Inc., Chatsworth, CA) and stored in NTA column elution buffer. This buffer (0.2 M imidazole, pH 7.5, 50 mM KPO_4, 0.3 M KCl, 2 mM $MgCl_2$, 10% glycerol, 0.1% CHAPS, 1 mM PMSF, 50 μM ATP, 5 mM BME) proved to be the best buffer to prevent MCAK aggregation and was used as the basis for both the gel exclusion chromatography and the sucrose gradient analysis.

Gel exclusion chromatography was performed on a Sepharose Cl6B (Pharmacia Chemical Co., Piscataway, NJ) using the following standards (Sigma Chemical Co.): thyroglobulin, apoferritin, β-amylase, alcohol dehydrogenase, and BSA. Calibration of the R_s was performed using values for the viscosity-based Stoke's radii (Horiike et al., 1983; de Haen, 1987), with the exception of yeast alcohol dehydrogenase for which only the frictional-based R_s was known (Buhner and Sund, 1969). Molecular weights were calculated using mol wt = $6\pi S_{20,w} N_A R_s \eta$ and the $S_{20,w}$ was estimated using sucrose density gradients and the same standards. CHO-K1 cells were removed from plates using EDTA and lysed in the same buffer used for the Ni column elution except the concentration of CHAPS was raised to 1% to facilitate lysis. The lysate was centrifuged for 100,000 *g* for 1 h at 4°C, and then the lysate was used for sucrose density gradient centrifugation or size exclusion chromatography in parallel with standards. BExp-MCAK and CHO-MCAK fractions were run on 4–12% gradient gels (Novex) and then scanned on a UMAX scanner and intensities were quantified using NIH Image (v. 1.61). CHO-MCAK was detected using Western immunoblots and quantified in a similar manner.

Preparation of Deletion Constructs

The GFP coding region from pTU65 (Chalfie et al., 1994) was fused to the MCAK coding region by recombinant PCR. This construct was cloned into the NotI sites of pOPRSVICAT (Stratagene, La Jolla, CA) eukaryotic expression vector (GFP-MCAK). Construct GFP-ΔN-MCAK was prepared from a FokI to AvrII digest of GFP-MCAK relegated with an oligo linker that replaces amino acids 1–136 with YK-GPG-PR (underlined residues are from the GFP sequence). Construct GFP-MCAK-ΔCC is a double digest of BlpI and EcoNI, subsequently filled in and relegated. This results in a deletion of residues 564–702 with the addition of a small out-of-reading frame product to the COOH end of the deletion construct. This excises the predicted coiled-coil domain of MCAK, and the out-of-reading frame translation product has zero predicted probability of coiled-coil formation (Lupas et al., 1991). Construct GFP-MCAK-ΔC was prepared by a single BclI digest, which was filled in and blunt ligated, resulting in out-of-reading frame stop codons after translation through the junction. Construct GFP-MCAK-ΔC results in a deletion of residues 647–702 with the addition of RSARL to the COOH end of the translation product. The numbering for the deleted residues described above corresponds to the residues of the MCAK peptide sequence (these sequence data are available from GenBank/EMBL/DDBJ under accession number U11790), not that of GFP-MCAK. Motorless GFP-MCAK was prepared from GFP-MCAK, which was digested with ClaI and Bpu 1102 I, filled in with T4 polymerase, blunt ligated, and then sequenced to verify the reading frame.

Cell Culture, Immunofluorescence, and Transfections

CHO cells were cultured as described in Wordeman and Mitchison (1995). 1 d before transfection, cells were plated at low density onto 12-mm coverslips. Cells were transfected for 3–6 h using the MBS mammalian transfection kit (Stratagene). Transfected cells were fixed either 16–24 h or 70 h after transfection for 3 min in −20°C MeOH plus 1% PFA. This fixation produced the most consistent MCAK labeling pattern from experiment to experiment. When large numbers of labeled cells were needed for quantitation, a 100-mm^2 dish was transfected for 16 h and the GFP-transfected cells were sorted using a FACStar® cell sorter (Cell Analysis Facility, Department of Immunology, University of Washington School of Medicine, Seattle, WA). Sorted cells were plated and fixed as described. Cells were

labeled with affinity-purified rabbit anti-MCAK, DM1α (mouse anti-tubulin; Sigma Chemical Co.), or human CREST sera (SH; a gift of Dr. B.R. Brinkley, Baylor College of Medicine, Houston, TX). Coverslips were washed in PBS plus 1 μg/ml Hoescht to label the DNA. Coverslips were observed using a Nikon FX-A photomicroscope and photographed using Kodak Technical Pan film. In some cases coverslips were analyzed using a confocal microscope (MRC 500; Bio-Rad Laboratories, Hercules, CA). For projected Z-series, between 35 and 50 0.2-μm sections were scanned and projected. In some cases, the projections were processed and viewed using Confocal Assistant software (v. 4.02). Negatives were scanned using a Nikon Coolscan II and overlaid using Photoshop 3.0 (Adobe Systems Inc., Mountain View, CA).

Antisense-induced Downregulation of MCAK

Fully substituted phosphorothioate oligos were purchased from Operon Technologies, Inc. (Alameda, CA) AS1 (5′-AAGCGACTCCATGGGCTCGGG-3′), AS2 (5′-GAGCTCAAGCCAGCCTGGTCC-3′), AS3 (5′-CTCTCCCAGAGCCTGCTT-3′), and RC1 (5′-AGGTGGCAGAATCGGCCTGCC-3′) were tested in an in vitro transcription/translation system (Promega Corp., Madison, WI) using [S^{35}]methionine. Construct pMX403 (MCAK in pBluescript II), T3 polymerase, and 10× mol/mol oligo to DNA template was added to the reaction. The reaction products were run on a 7% gel (Novex), dried, and then exposed overnight to Kodak X-Omat film.

For each scrape-loading experiment, five 150-cm^2 plates of CHO cells were used. Mitotic cells were collected by mitotic shake-off and replated onto 35-mm^2 dishes for 3 h. After the cells had attached to the plate, the cultures were rinsed and then scraped in the presence of 100 pmol oligo in 100 μl serum-free MEMα. When necessary, 1 nmol digoxigenin-11-UTP (Sigma Chemical Co.) was added to the oligo-containing solution. Scraped cells were resuspended in 4 ml of media and replated onto four 12-mm-diam coverslips. Cells were cultured for 16–48 h and scored immunofluorescently for the presence of MCAK-free cells. Cells were double-labeled with rabbit anti-MCAK and either DM1α (Sigma Chemical Co.) or anti-digoxin (Jackson Immunoresearch Laboratories, Inc., West Grove, PA) antibodies.

Live Imaging

Before live observation, FACsorted® GFP-positive cells were plated on round coverslips (22-mm No. 1; Fisher Scientific Co., Pittsburgh, PA) and cultured at 37°C and 5% CO_2 in Ham's F12 nutrient mixture (Gibco Laboratories, Grand Island, NY) supplemented with 10% FBS (Hyclone, Logan, UT) and pen/strep (Gibco Laboratories). For live observation, coverslips were mounted in a cell chamber/temperature controlled stage (Brook Industries, Lake Villa, IL) and cells were maintained at 37°C, with the temperature feedback probe positioned within 1 mm of the coverslip surface. The cell chamber was perfused with F12 medium containing 10% FBS, 20 mM Hepes, 4 mM $NaHCO_3$, pen/strep, and 1 mM ascorbic acid to combat cellular photo damage resulting from free radicals.

Live observations were made using a Nikon Diaphot inverted microscope equipped with a 75W xenon lamp for fluorescence. For live imaging, the excitation light was attenuated to 10% transmission with a neutral density filter. For green fluorescent protein (GFP) fluorescence, the light was filtered with a FITC filter set (No. 31001; Chroma Technology Corp., Battleboro, VT). A Nikon PlanApo 100× NA 1.40 oil immersion objective was used for all time-lapse imaging. Time-lapse images were acquired at 10- or 20-s intervals using a PentaMax cooled CCD camera (Princeton Instruments, Princeton, NJ) controlled by MetaMorph software (v. 3.0; Universal Imaging Corp., West Chester, PA). Exposure times were generally between 200 and 500 ms.

Results

Molecular Analysis of MCAK

Genomic DNA blots indicate that MCAK is encoded by a single structural gene (Fig. 1 *A*, *1*). Probes synthesized from the NH_2-terminal and COOH-terminal regions of MCAK, exclusive of the motor domain, hybridize to a single band in both HindIII and BamHI digests of genomic DNA. Affinity-purified anti-MCAK polyclonal sera immunoprecipitates a single 90-kD band from high speed supernatants of [S^{35}]methionine-labeled CHO cell lysates (Fig. 1 *A*, *2*). This suggests that the bulk of MCAK protein in CHO cells is not associated with any other protein subunits.

To confirm this the hydrodynamic properties of baculovirus produced 6× histidine-tagged recombinant CHO cell MCAK were determined by gel filtration on a Sepharose CL6B column. This indicated that BExp-MCAK has a Stokes radius of 6.9 nm. This was determined using a plot of viscosity-based Stokes radii rather than frictional coefficient-based Stokes radii for the standards (Horiike et al., 1983). Our value is in close agreement with the 6.95 Stokes radius determined for the structurally similar kinesin-related protein KIF2 (Noda et al., 1995). The sedimentation coefficient for BExp-MCAK was determined to be 5.3 S by sucrose density gradient centrifugation. The empirically determined R_s and $S_{20,w}$ were used to calculate a molecular weight of 153,000 D for native BExp-MCAK. This suggests that baculovirus-expressed MCAK is a homodimer since the amino acid sequence of MCAK predicts a protein of 79,000 D. The relatively large value for R_s and small value for $S_{20,W}$ suggests that BExp-MCAK is not a spherical protein. In fact, the f_e/f_o for BExp-MCAK can be calculated to be 1.12 suggesting that the protein has an axial ratio of ~3. Thus, it is likely that native MCAK in solution is an oblate ellipse. The electron micrographs of circular KIF2 molecules by Noda et al. (1995) support this idea and our results for BExp-MCAK are in good accordance with the previously reported hydrodynamic measurements of baculovirus-expressed KIF2.

To confirm that MCAK in CHO cells was a homodimer, size exclusion chromatography and sucrose density gradient centrifugations were performed in parallel with high speed supernatants of lysed CHO cells. The results are shown in Fig. 1 *B*, *1* and *2*. CHO MCAK was detected using Western blots. We found that the bulk of MCAK in CHO cells exhibited similar hydrodynamic properties as purified BExp-MCAK. The values obtained for R_s and $S_{20,W}$ were 7.5 nm and 4.9 S, respectively. We presume that the larger Stokes radius determined for cellular MCAK is not indicative of associated cellular proteins because the sedimentation coefficient is comparatively smaller. The molecular weight for cellular MCAK is estimated to be 157,600 D. Hence, the bulk of cellular MCAK exists in the form of a homodimer with no other detectable associated proteins.

MCAK Domains Required for Centromere and Microtubule Binding

A construct consisting of the protein coding region for GFP fused to the 5′ end of the coding region of CHO MCAK was transfected into CHO-K1 cells (Fig. 1 *C*, *GFP-MCAK*). Full-length GFP-MCAK is seen diffusely distributed throughout the cytoplasm and the nucleus of transfected interphase cells (Fig. 1 *E*, *a*). During mitosis GFP-MCAK redistributed to become associated with the mitotic centromeres, and, to a lesser extent, the spindle poles (Fig. 1 *D*, *a*). The spatial distribution of full-length GFP-MCAK was indistinguishable from that seen when

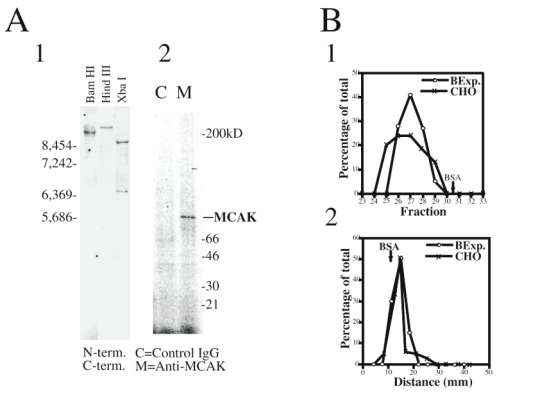

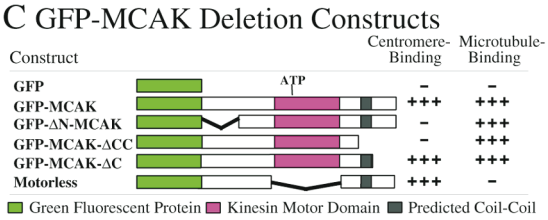

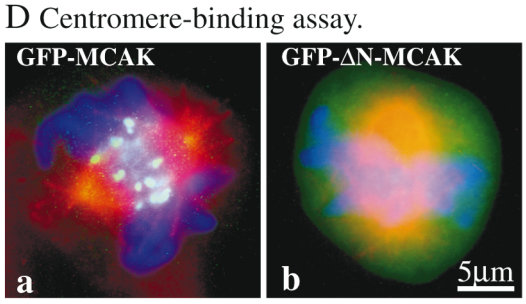

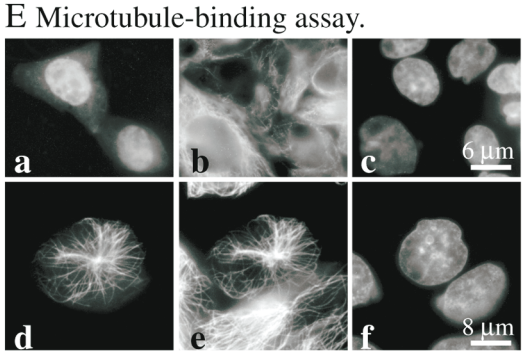

Figure 1. Molecular and functional analysis of MCAK. (*A*) MCAK is a homodimer, encoded by a single gene with no associated subunits. (*1*) Genomic CHO-K1 DNA digested with BamHI, HindIII, or XbaI and hybridized to P^{32}-labeled probe synthesized from DNA sequences for the NH_2-terminal or COOH-terminal regions of MCAK, exclusive of the motor domain. Hybridizations of the combined NH_2-terminal and COOH-terminal regions indicate that MCAK is encoded by a single gene. (*2*) Cell lysates from [S^{35}]methionine-labeled CHO-K1 cells immunoprecipitated with affinity-purified anti-MCAK polyclonal antibodies (*M*) or nonimmune purified IgG. (*B*) Hydrodynamic analysis of MCAK (*1*) Gel exclusion chromatography of Baculovirus-expressed MCAK (*BExp-MCAK*) and CHO lysate superimposed. Gel filtration standards have been omitted for clarity. CHO MCAK was detected by Western immunoblot. (*2*) Sucrose density gradient of BExp-MCAK and CHO lysate run in parallel and superimposed. Standards have been omitted for clarity. Intensities of scanned gels and blots have been plotted against the fraction number (in the case of *1*) and the distance migrated (in the case of *2*). MCAK in CHO cell lysates behaves similarly to purified His-tagged MCAK expressed in the baculovirus expression system. (*C*) GFP-MCAK deletion mutant analysis. NH_2-terminal fusion of GFP to MCAK does not affect binding of expression fusion protein to mitotic centromeres during cell division. However, deletion of the NH_2 terminus of MCAK or the COOH terminus, inclusive of the predicted coiled-coil domain, abolishes centromere binding. Cells lysed before fixation in the absence of ATP exhibit rigor binding of MCAK to microtubules. Constructs were assayed for microtubule-binding capability using this assay. (*D*) Examples of centromere-binding assay. (*a*) Full-length GFP-MCAK expressed for 16 h in CHO cells exhibits a spindle localization pattern indistinguishable from endogenous protein. (*b*) GFP-ΔN-MCAK fails to localize to mitotic centromeres. GFP-MCAK and GFP-ΔN-MCAK, *green*; microtubules, *red*; DNA, *blue*. (*E*) Microtubule-binding assay. (*a–c*) Normal interphase CHO cells transfected with GFP-MCAK and fixed 16 h later. Diffuse cytoplasmic and nuclear label is evident. (*a*) GFP-MCAK. (*b*) Microtubules. (*c*) DNA. (*d–f*) Interphase cell transfected with GFP-MCAK and lysed before fixation. Constructs were assayed for the ability to bind microtubules in this manner. (*d*) GFP-MCAK. (*e*) Microtubules. (*f*) DNA. Bars: (*D*) 5 μm; (*E*, *a–c*) 6 μm; (*E*, *d–f*) 8 μm.

using antibodies to detect endogenous MCAK (Wordeman and Mitchison, 1995). This result suggests that the inclusion of GFP on the NH_2 terminus of the molecule does not interfere with MCAK targeting in vivo.

Centromere-binding was abolished in constructs with an NH_2-terminal deletion of MCAK (Fig. 1 *C*, *GFP-ΔN-MCAK*; Fig. 1 *D*, *b*). Additionally, centromere binding was also abolished if a region inclusive of the predicted coiled-coil (PAIRCOIL) in the COOH-terminal tail of MCAK was deleted (Berger et al., 1995). These results suggest that the binding of MCAK to the centromere may be dependent on the NH_2 terminus of the protein and also on the quaternary structure of the protein. We constructed a motorless version of MCAK that consisted of the NH_2- and COOH-terminal tails fused in reading frame. This GFP-construct (Fig. 1 *C*, *Motorless*) bound centromeres, centrosomes, and spindle midbodies (in a manner similar to endogenous MCAK). Hence, targeting of MCAK to different regions of the mitotic spindle is not dependent on the motor domain.

Cells lysed in a microtubule-stabilizing buffer before fixation exhibit a redistribution of endogenous MCAK label. MCAK remains associated with centromeres and centrosomes but additional cytoplasmic MCAK becomes bound to existing microtubule arrays in both interphase and mitotic cells. We used this simple assay to test the microtubule-binding activity of the deletion constructs. The results of such an assay are shown in Fig. 1 *E*. Full-length GFP-MCAK redistributes to microtubules during preextraction (Fig. 1 *E*, *d–f*). Positive microtubule-binding always requires an intact motor domain in all deletions we have examined. As expected, the motorless construct of MCAK does not bind microtubules in this rigor binding assay (Fig. 1 *C*).

MCAK Is Required for Chromosome Segregation Specifically at Anaphase

Populations of transfected mitotic cells were examined to determine whether any of the GFP-MCAK deletion con-

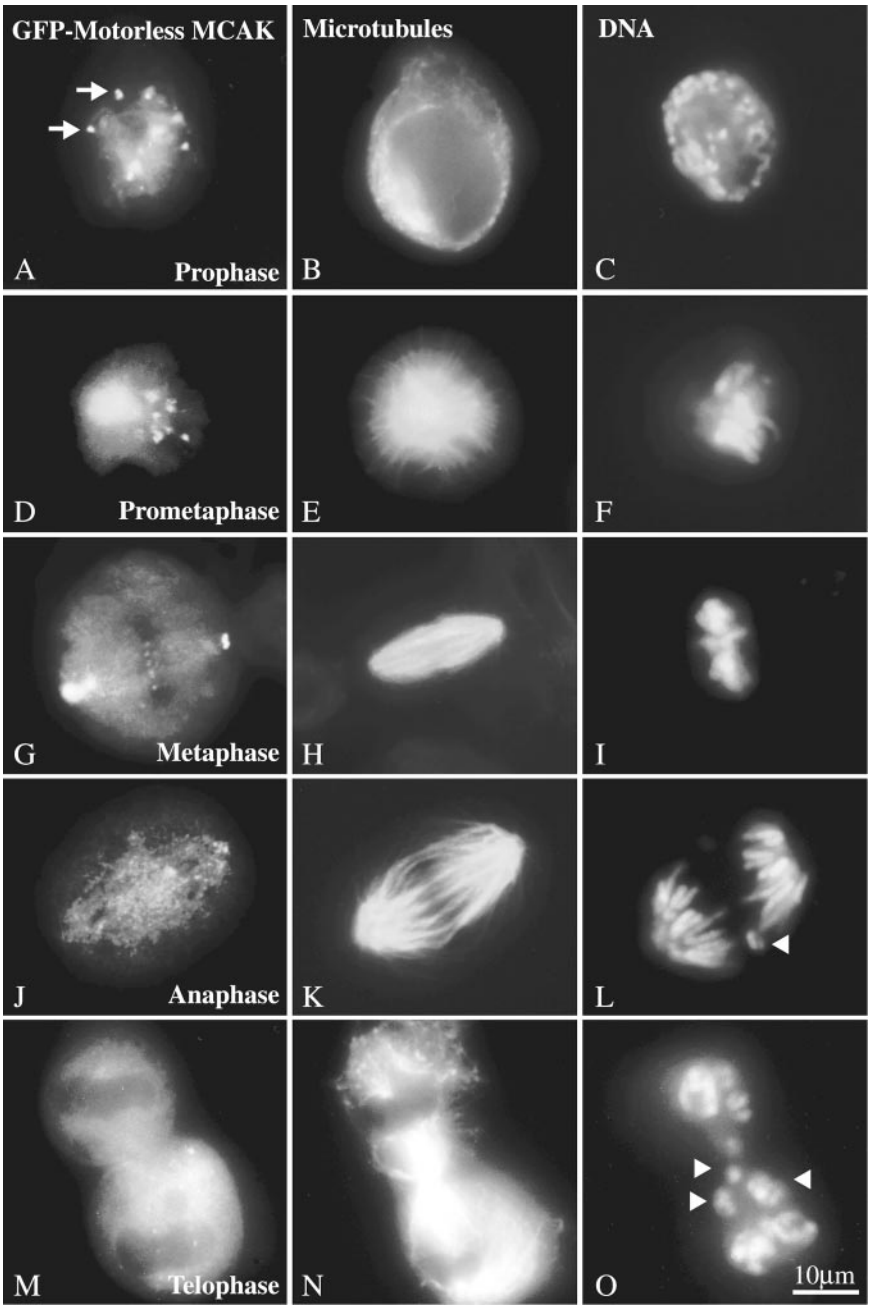

Figure 2. The GFP-motorless deletion exhibits a lagging chromosome phenotype at the onset of anaphase. Like endogenous MCAK, motorless GFP-MCAK localizes to nuclei, mitotic centromeres, and centrosomes. (*A*, *D*, *G*, *J*, *M*) Motorless GFP-MCAK; (*B*, *E*, *H*, *K*, *N*) microtubules; (*C*, *F*, *I*, *L*, *O*) DNA. GFP-motorless appears on centromeres (*A*, *arrows*) at prophase (*A–C*). Spindle assembly and chromosome distribution appear to be unaffected through prometaphase (*D–F*) and metaphase alignment (*G–I*). Lagging chromosomes (*arrowheads*) appear during anaphase (*J–L*) and telophase (*M–O*). Bar, 10 μm.

structs exerted a dominant-negative effect on microtubule-dependent events. The GFP-motorless construct exhibited a dominant-negative lagging chromosome phenotype at the onset of anaphase chromosome movement (Table I). Fig. 2 shows the localization of the motorless construct throughout mitosis (Fig. 2, *left-hand column*). The presence of the motorless construct has no effect on spindle microtubules (Fig. 2, *middle column*) or spindle assembly. However, after anaphase onset chromosomes are left behind during chromosome-to-pole movement (Fig. 2, *right-hand column*). Immunofluorescence and confocal microscopy indicate that the sister chromosomes have separated (Fig. 3). A confocal stacked Z-series of a GFP-motorless–containing telophase cell (Fig. 3 *C*) or a merged, stacked Z-series of GFP-motorless (*green*) and CREST label (*red*) all support the conclusion that the lagging sister chromosomes have separated (Fig. 3 *D*). Note that GFP-motorless localizes to centromeres (Fig. 3, *arrows*), spindle poles (Fig. 3, *C* and *D*, *filled arrowheads*), and the spindle midbody (Fig. 3, *C* and *D*, *open arrowheads*). At longer time points (70 h) after transfection, the motorless construct exhibited the same defect. By this time multinucleate interphase cells containing micronuclei were quite evident in the culture. As expected, in these long-term transfectants the motorless construct has no effect on the mitotic spindle as it does not bind microtubules. Neither full-length GFP-MCAK, nor the NH_2- or COOH-terminal deletions had any obvious effect on the cells within 16 to 24 h after transfection. However the motor-containing constructs manifested a pseudoprometaphase arrest phenotype by 70 h after transfection because of spindle microtubule disruption (see below).

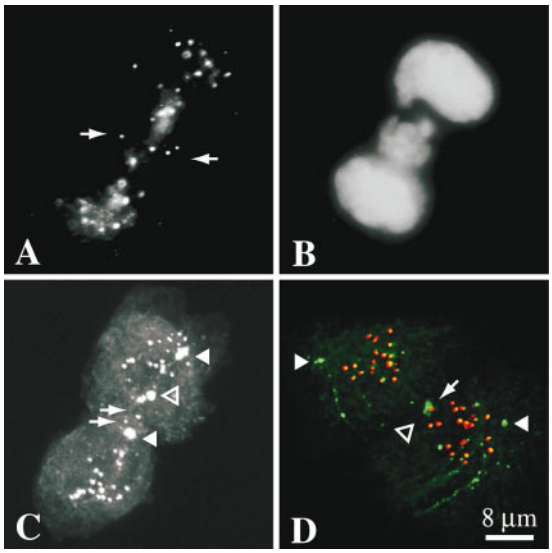

Figure 3. Lagging chromosomes have undergone sister chromosome separation. (*a* and *b*) Fluorescence microscopy of a telophase cell transfected with GFP-motorless. Single dots of centromere-bound GFP-motorless (*a*) are visible (*arrows*). (*b*) DNA. (*c*) Confocal projected Z-series of a motorless GFP-motorless transfectant in late telophase. GFP-motorless (shown) exhibits lagging centromeres (*arrows*), spindle poles (*arrowheads*), and midbody (*open arrowhead*). In the confocal micrograph, one daughter cell has rotated, bringing the centrosome between the cleavage furrow and the chromosomes. Single centromeres can be seen in the vicinity of the cleavage furrow (*arrows*). (*d*) Confocal projected Z-series of a late telophase cell transfected with GFP-motorless. The merged image consists of CREST sera label (*red*) and GFP-motorless (*green*). Spindle poles (*filled arrowheads*) and midbody (*open arrowhead*) are also indicated. Several lagging centromeres are visible with one (*arrow*) residing close to the cleavage furrow. All centromeres appear to have separated. Bar, 8 μm.

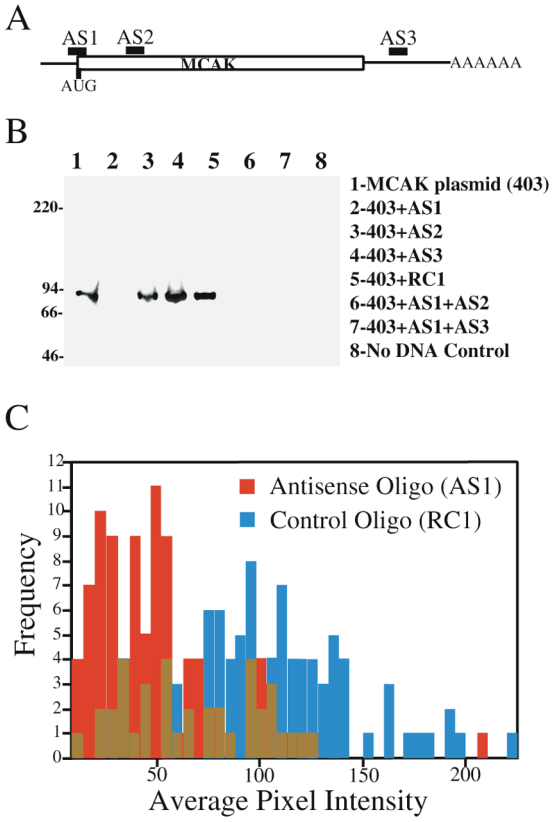

Figure 4. Antisense-induced depletion of MCAK protein. (*A* and *B*) Potency of phosphorothioate oligos for the inhibition of MCAK translation in vitro. (*A*) Diagram of the location of three antisense oligonucleotides within MCAK mRNA transcript. *AS1*, start codon; *AS2*, within the amino acid coding region; *AS3*, within the 3′ untranslated region. (*B*) Transcription/translation of MCAK in pBluescript II SK$^-$ (construct 403) using T3 polymerase and [S^{35}]methionine. Oligos were added to the reaction in a 10-fold excess over DNA template. Oligonucleotide AS1 was the only oligo effective in inhibiting translation in vitro. (*C*) AS1-induced depletion of endogenous MCAK. 100 pmol of antisense (*AS1*) or control (*RC1*) oligos were scrape-loaded into CHO cells in combination with digoxigenin-UTP. Digoxigenin-positive cells were scored immunofluorescently for MCAK intensity.

If the GFP-motorless phenotype is due to the competitive replacement of functional endogenous MCAK at subcellular locations by the expressed motorless protein, then simple depletion of endogenous MCAK should result in a similar phenotype. To test this hypothesis, we experimentally depleted endogenous MCAK protein in logarithmically growing CHO cells. Three different fully substituted phosphorothioate oligos complimentary to different regions of the MCAK coding sequence (Fig. 4 *A*) were prepared. In addition a control phosphorothioate oligo was synthesized from the randomized sequence of AS1 (see Materials and Methods). The effectiveness of these oligos was tested in vitro using a coupled transcription/translation kit. We determined that an antisense oligo directed against the regions surrounding the start codon of MCAK (AS1) was the only oligo effective in inhibiting the synthesis of MCAK protein in vitro (Fig. 4 *B*). To determine if AS1 was effective in vivo in depleting MCAK protein, we scrape-loaded AS1 and RC1 into logarithmically growing CHO cells (see Materials and Methods). Scrape-loaded cells were identified by co-loading the cells with digoxigenin-UTP and labeling the cells with an anti-digoxin mAb (see Materials and Methods). Endogenous MCAK fluorescence was measured (see Materials and Methods) and plotted on a histogram (Fig. 4 *C*). MCAK levels in tissue culture cells are inherently variable, with higher levels generally measurable in G2 cells versus G1 (not shown). This is reflected in the broad distribution of label intensity in the cells loaded with control oligo and is indistinguishable from the distribution seen in unloaded cells (not shown). Nevertheless, in AS1-loaded cells, the level of endogenous MCAK label is significantly reduced. Significant numbers of interphase and mitotic cells can be identified in which the level of MCAK protein is below our level of detection by immunofluorescence light microscopy. Examples of such mitotic cells are shown in Fig. 5. MCAK-depleted mitotic cells progress through mitosis with no discernible problems until metaphase after which time-lagging chromosomes are seen. This phenotype closely resembles that seen in cells transfected with the GFP-motorless construct.

Spindle stage profiles of AS1- and RC1-loaded cells and motorless transfectants are compared in Fig. 6 *A*. The pro-

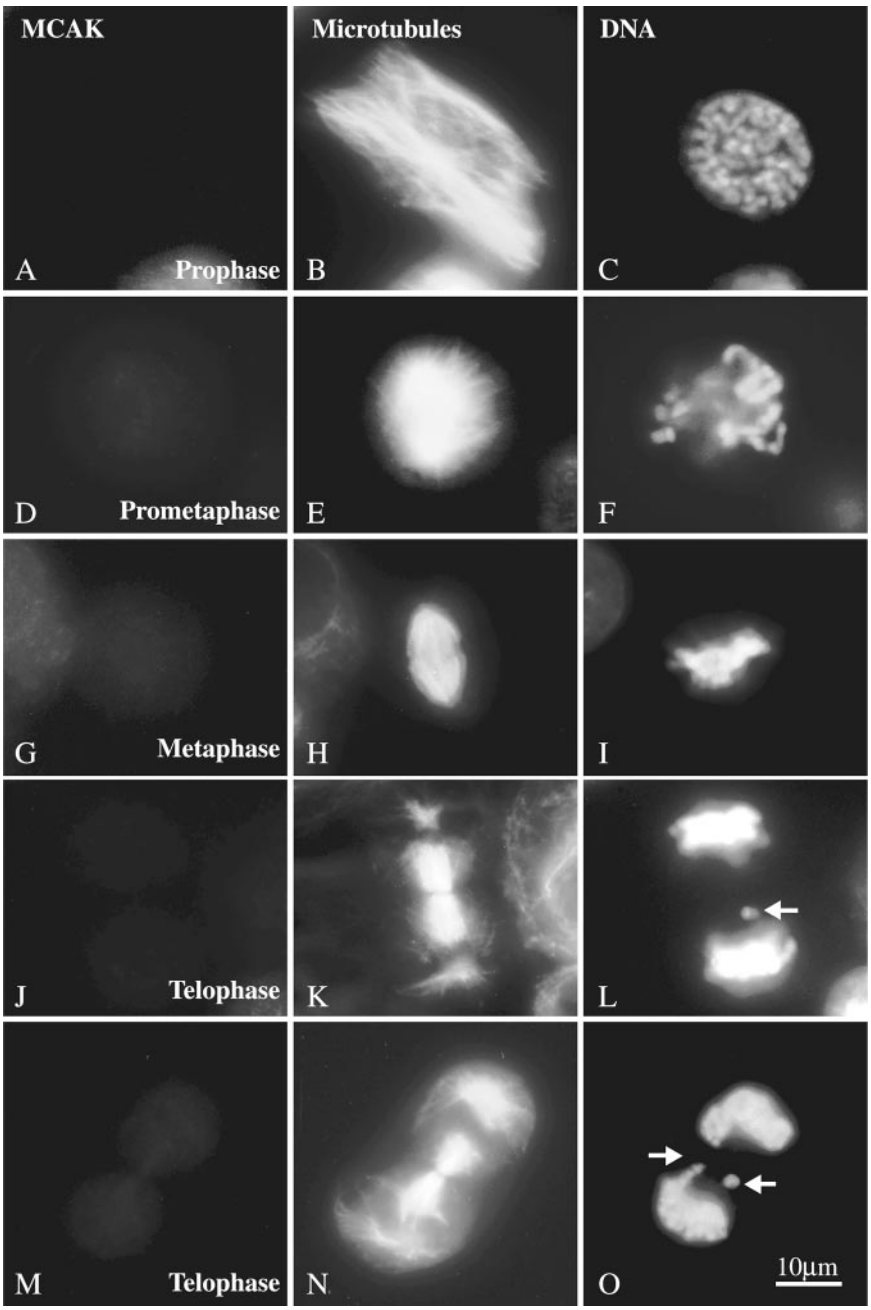

Figure 5. Effect of endogenous MCAK depletion on chromosome segregation. Mitotic cells triple-labeled with anti-MCAK (*A*, *D*, *G*, *J*, *M*); anti-tubulin (*B*, *E*, *H*, *K*, *N*); and Hoechst (*C*, *F*, *I*, *L*, *O*). Endogenous MCAK was below the level of detection by immunofluorescence microscopy. Spindle assembly and chromosome alignment appeared normal during prophase (*A–C*), prometaphase (*D–F*), and metaphase (*G–I*). However, many telophase cells (*J–O*) with lagging chromosomes (*arrows*) were identified. Bar, 10 μm.

files of spindle stages for AS1-loaded cells and motorless transfectants were not significantly different from RC1-loaded cells and GFP transfectants. This supports the hypothesis that MCAK is dispensable for mitotic spindle stages before anaphase in tissue culture cells. Alternatively, anaphase chromosome movement may be the mitotic stage that is most sensitive to partial MCAK depletion. The MCAK-related defect manifests itself after the metaphase-to-anaphase transition as lagging chromosomes. This is shown in Fig. 6 *B*. Although a baseline of lagging chromosomes (and multinucleate cells) is observed in any transformed cell line, the application of the AS1 oligo or the transfection of motorless GFP-MCAK doubles or triples, respectively, the incidence of this defect in CHO cells. The requirement for MCAK during anaphase chromosome segregation is consistent with the observation that it is the only presently identified microtubule-dependent motor molecule that remains associated with the mitotic centrosome through telophase (Wordeman and Mitchison, 1995).

The Mechanism Underlying the Lagging Chromosome Defect

Spindle profiles and DNA analysis indicate that the chromosomes in GFP-motorless cells are capable of congressing to the metaphase plate during prometaphase. However, it is quite possible that a more subtle defect in metaphase alignment may delay the progression of some chromosomes into anaphase. This defect would be expected

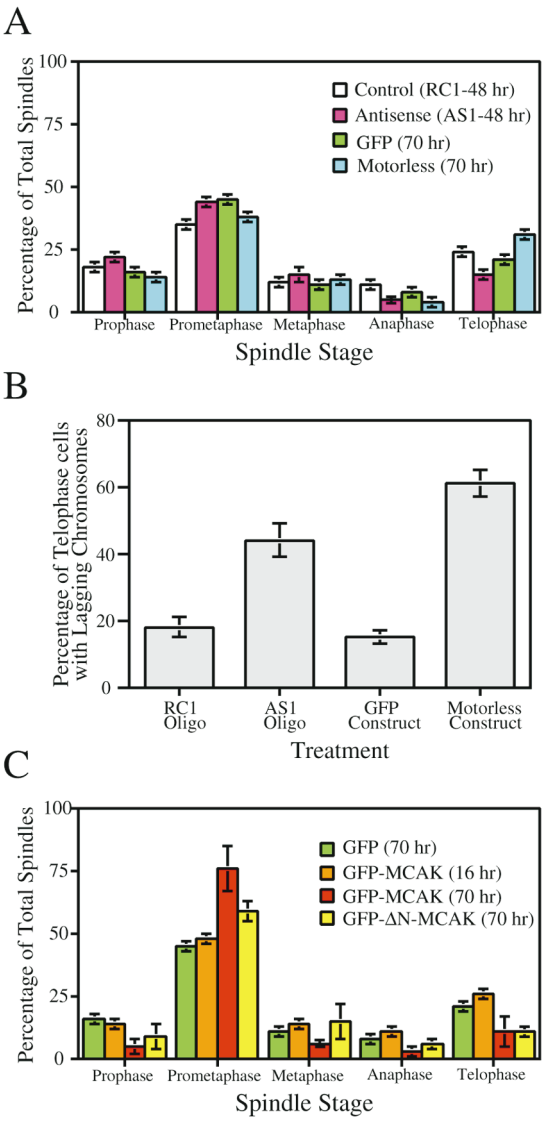

Figure 6. Spindle profiles of transfectants and antisense-loaded mitotic cells. (*A*) Spindle profiles of control (*RC1*) and antisense (*AS1*) loaded cells (48 h after loading) were not significantly different from each other or from control GFP-transfected or GFP-motorless–MCAK transfected cells (70 h after transfection). *Inset*, Spindle stages based on live video analysis. *P*, prophase; *PM*, prometaphase; *M*, metaphase; *A*, anaphase. (*B*) Telophase cells of AS1-loaded and GFP-motorless–transfected cells have significantly increased numbers of lagging chromosomes relative to control telophase cells. (*C*) Transfected GFP-MCAK constructs that contain the MCAK motor domain induce mitotic arrest in a prometaphase-like configuration after 70 h of expression. For scrape-loaded cells the number of mitotic cells scored is >1,000; in the case of transfected cells the number of mitotic cells scored is >300.

to manifest itself in only a few chromosomes, since only a few are lagging in either MCAK-depleted or GFP-motorless–containing cells. Stacked Z-series were projected for normal metaphase cells (Fig. 7, *A–C*), GFP-MCAK–containing (Fig. 7, *D* and *E*), and GFP-motorless–containing metaphase cells (Fig. 7, *F–G*). The projected Z-series are shown in Fig. 7 for merged images of CREST label (*red*) or anti-MCAK immunofluorescence (Fig. 7, *A–C*, *green*), GFP-MCAK (Fig. 7, *D* and *E*, *green*) or GFP-motorless (Fig. 7, *F-H*, *green*). No significant differences were observed in the qualitative appearance of the metaphase chromosomes. All sister-chromosome pairs appeared to be longitudinally oriented on the metaphase plate and under tension, as suggested by the increased distance between the sister-centromeres compared with what is seen at earlier mitotic stages (data not shown). This was unambiguous when the Z-series projections were viewed as looped movies using Confocal Assistant version 4.02 (not shown).

One difference between the endogenous MCAK (and GFP-MCAK, not shown) distribution and GFP-motorless is shown in Fig. 8. In metaphase cells, endogenous MCAK and GFP-MCAK (not shown) appears to stretch between the centromeres (Fig. 8, *A* and *B*, *large brackets*). However, in metaphase cells that have been transfected with GFP-motorless, the GFP label is often compressed or irregularly clumped between the sister centromeres (Fig. 8, *C* and *D*, *small brackets*). This staining pattern is evident despite the fact that the inter-centromere distance between control and GFP-motorless sister centromeres is not significantly different as determined by the paired *t* test (not shown). This suggests that the MCAK binding sites are found on an extensible matrix between the sister centromeres. This matrix becomes stretched toward the centromere/corona when the MCAK motor domain is intact. Presently, light microscopic immunocytochemistry does not have the resolution to determine if this is due to the interaction of MCAK with microtubule ends.

In a cell in which the modal number of chromosomes is 21 (Deaven and Petersen, 1973), it is within the realm of possibility that a subtle alignment defect could affect only one or two sister chromatids and not be distinguishable. For this reason we observed the anaphase defect occurring in living cells to gain some insight into how it comes about. A cell transfected for 48 h with GFP-MCAK is shown progressing from metaphase through anaphase in Fig. 9, *A–H*. This cell was chosen as a control based on two criteria: (*1*) the cell expressed very low levels of GFP-MCAK and therefore was not subject to the MCAK overexpression defect; (*2*) the chromosomes all segregated normally (there is a baseline level of abnormal segregation in any cell line). The live cell shown in Fig. 9, *I–P* has been expressing the GFP-motorless construct for 48 h. After cytokinesis both daughter cells had several lagging chromosomes. Timing in seconds was started at a point in metaphase just before the onset of anaphase for both cells. In both cells, prometaphase and metaphase oscillations appear identical in amplitude and speed (not shown). All bi-oriented chromosomes oscillated at metaphase (not shown). At the onset of anaphase, all the sister chromatids in the GFP-MCAK cell separated (Fig. 9 *B*). One centromere (*1*) of a sister chromatid pair (*1*, *1′*) manifested a temporary reversal in direction during anaphase (Fig. 9 *D*) that did not impair anaphase chromosome segregation. Such anaphase oscillations have been previously described (Skibbens et al. 1994). In Fig. 9, *F–H*, a second centromere (*2*) comes into focus and appears to be lagging slightly but not grievously. In the cell transfected with GFP-motorless, most but not all of the sister chromatids separate (Fig. 9 *J*). One pair (*1*, *1′*) that are in the plane of focus continue to

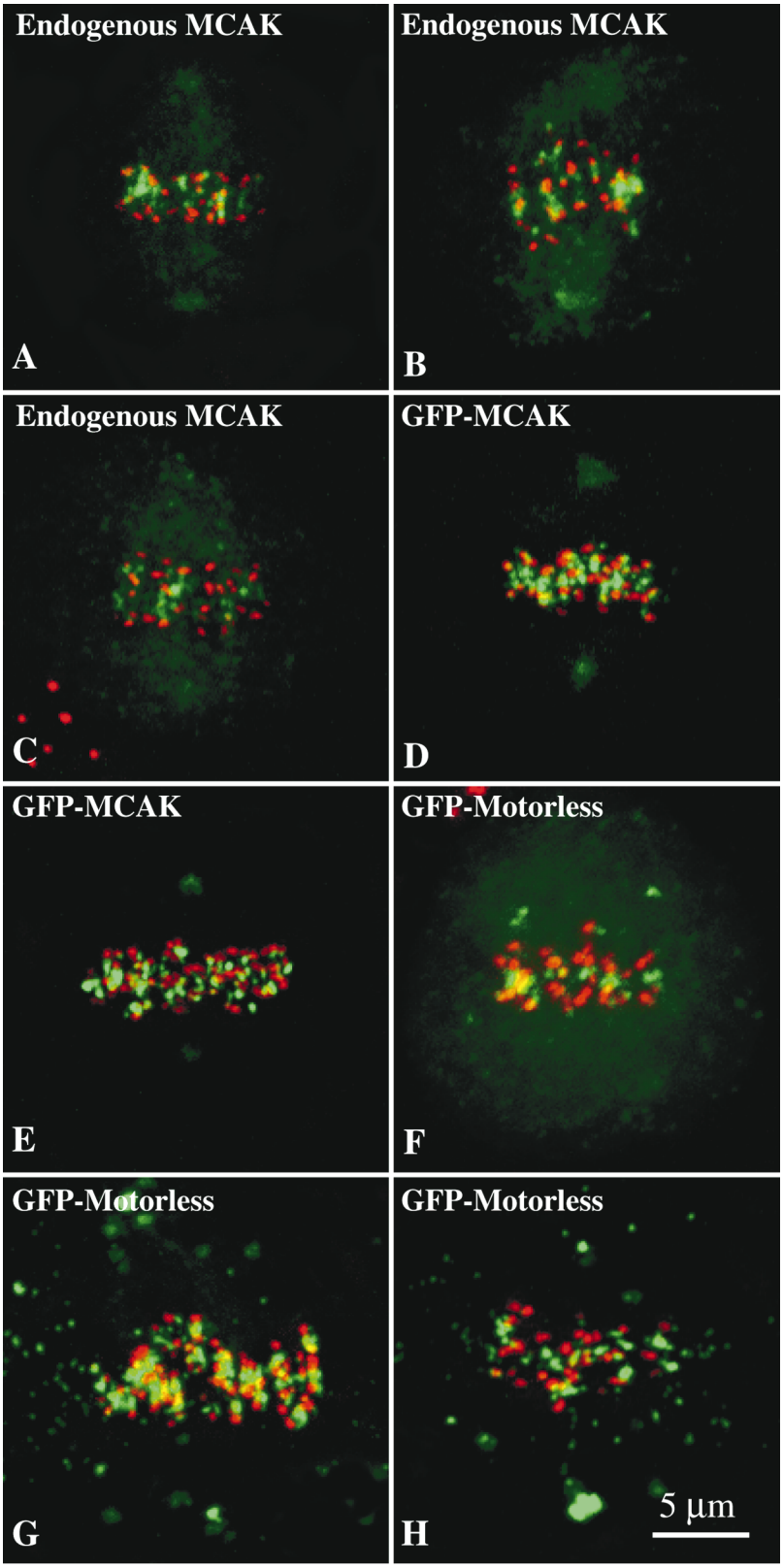

Figure 7. Metaphase alignment in GFP-motorless-transfected cells. Projected confocal Z-series of merged images of metaphase cells double-labeled with CREST sera (*red*) and either endogenous MCAK (*A–C*, *green*); GFP-MCAK (*D* and *E*, *green*); or GFP-motorless (*F–H*, *green*). Metaphase alignment of GFP-motorless (*F–H*) does not differ substantively from control cells (*A–E*). Bar, 5 μm.

oscillate after the other chromosomes have separated (Fig. 9, *J–L*). These chromatids separate eventually (Fig. 9 *M*) but are unable to reach the other chromosomes at the respective spindle poles. Each sister chromosome (*1* and *1′*) becomes part of a number of lagging chromosomes that become obvious during telophase (Fig. 9, *O* and *P*). This result suggests that the lagging chromosome phenotype occurs due to delayed separation at the onset of anaphase.

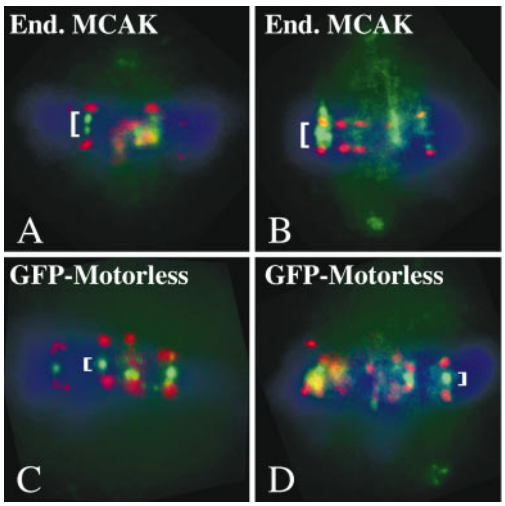

Figure 8. Metaphase distribution of MCAK differs slightly from GFP-motorless. Control metaphase spindles (*A* and *B*) showing endogenous MCAK label (*green*) and CREST label (*red*). GFP-motorless-transfected cells (*B* and *D*) showing GFP-motorless (*green*) versus CREST label (*red*). In control metaphase cells, MCAK appears to extend throughout the inner centromere regions (*A* and *B*; *large brackets*) whereas GFP-motorless consistently appears compressed (*C* and *D*; *small brackets*).

Long-Term MCAK Overexpression Disrupts Mitotic Spindle Microtubules

Populations of mitotic transfected cells were scored for mitotic stage, which is a reflection of the time required for each stage. Spindle profiles for control GFP alone and GFP-motorless transfectants are not significantly different from control spindles even after 70 h of expression (Figs. 1 *C*, and 6 *A*). Furthermore, after 16 h of expression, full-length GFP-MCAK has no significant effect on the spindle profile (Fig. 6 *C*). However, it can be seen that in cells that have been expressing GFP-MCAK for 70 h, a prometaphase arrest phenotype is manifest (Fig. 6 *C*). This prometaphase arrest does not appear to be dependent on centromere-associated protein because it is seen in conjunction with both the GFP-ΔN-MCAK (Fig. 6 *C*) and the GFP-MCAK-ΔCC

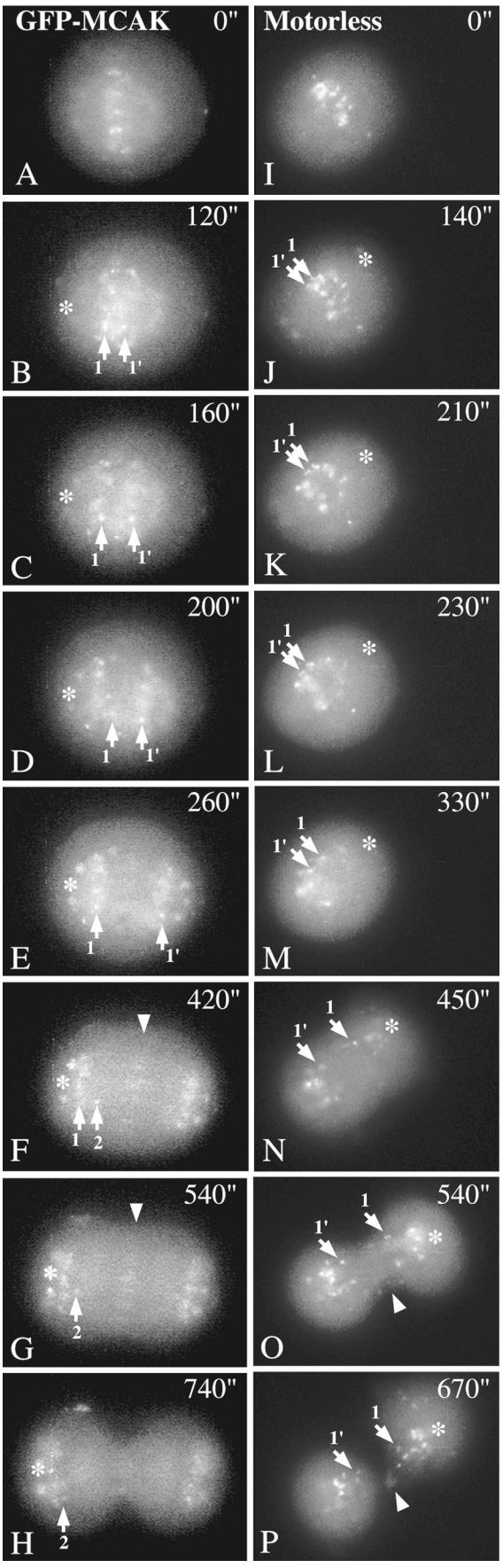

Figure 9. Live cell imaging of GFP-MCAK– and GFP-motorless–transfected cells. GFP-MCAK–transfected cells (*A–H*) were tracked from an arbitrary time at metaphase (*A*, *t = 0′′*) until telophase (*H*). All chromosomes in this cell segregated completely despite the fact that one centromere suffered a transient reversal (*D*; *1*) or anti-poleward oscillation during chromosome-to-pole movement. GFP-motorless–transfected cells (*I-P*) were tracked from an arbitrary point during metaphase (*I*, *t = 0′′*) to telophase (*P*). In this cell, one pair of sister centromeres (*1*, *1′*) fail to separate at the onset of anaphase (*K*) and continue to oscillate. Eventually the sister separate late (*M*), however, they never make it to the spindle pole. Both late-separating sister chromosomes end up lagging close to the cleavage furrow at cytokinesis (*O* and *P*). Other lagging centromeres that were not traced because they did not remain in the plane of focus throughout anaphase are also visible (*O* and *P*). Both GFP-MCAK and GFP-motorless appear on the spindle midzone during anaphase B (*F* and *G*, *arrowhead*; *O*, *arrowhead*).

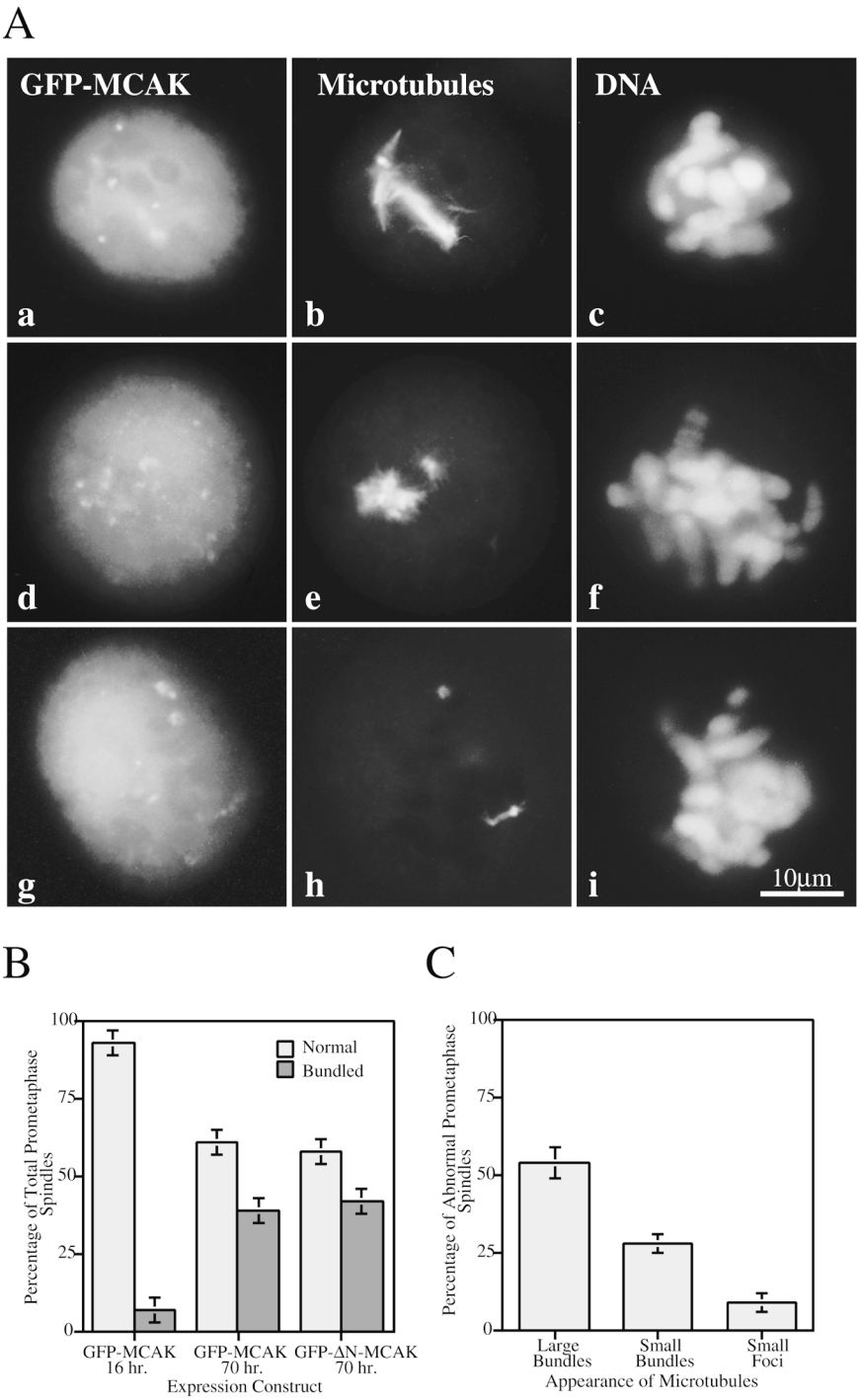

Figure 10. Pseudoprometaphase-arrest by MCAK overexpression results from spindle microtubule abnormalities. (*A*) Examples of typical prometaphase-arrested spindles. GFP-MCAK (*a*, *d*, *g*); microtubules (*b*, *e*, *h*); DNA (*c*, *f*, *i*). Spindles microtubules consist of large bundles (*a–c*); small bundles (*d–f*) or small to nonexistent foci of tubulin staining (*g–i*). (*B*) Characterization of prometaphase spindles in 16-h vs. 70-h GFP-MCAK and GFP-ΔN-MCAK transfectants. Significant increases in abnormal prometaphase spindles occur between 16 and 70 h after transfection. (n = 200 prometaphase cells.) (*C*) Quantitation of microtubule disappearance in pseudoprometaphase-arrested spindles (GFP-MCAK overexpression). (n = 150 abnormal prometaphase spindles.) Bar, 10 μm.

(not shown) constructs, both of which do not bind centromeres.

The microtubule phenotypes of the prometaphase-arrested transfectants is significantly altered from that seen in normal prometaphase cells. The microtubules appear bundled to varying extents (Fig. 10 *A*, *a–c*) and often the bundles appear to be unusually small (Fig. 10 *A*, *d–f*) or practically nonexistent (Fig. 10 *A*, *g–i*). This easily identifiable phenotype increases significantly from 16 to 70 h after transfection (Fig. 10 *B*). We have seen this phenotype appear by 70 h in all transfected deletion constructs that have an intact MCAK motor domain (Table I). Double label of CREST antigens and microtubules in these cells indicates that the attachment of chromosomes to the spindle does not appear to be compromised until the microtubules have almost completely disappeared (not shown). The proportion of pseudoprometaphase spindles exhibiting different microtubule abnormalities is shown in Fig. 10 *C*. This phenotype is consistent with MCAK exhibiting both a bundling and depolymerizing activity, that have both been described for structurally related kinesins (Noda et al., 1995; Walczak et al., 1996).

Table I. Mitotic Defects Induced by Mutant Constructs

Construct	16 h PT	70 h PT
GFP	None	None
GFP-MCAK	None	PPM
GFP-ΔN-MCAK	None	PPM
GFP-MCAK-ΔCC	None	PPM
GFP-MCAK-ΔC	None	PPM
Motorless	AD	AD

PPM, pseudoprometaphase; *AD*, anaphase defect; *PT*, posttransfection.

Discussion

Lagging chromosomes during anaphase are an easily assayed and therefore commonly reported mitotic defect. However, in most cases, the mechanisms that give rise to lagging chromosomes are unknown. Lagging chromosomes can be caused by asbestos fibers (Hersterberg and Barrett, 1985), elevated *ras* p21 expression (Hagag et al., 1990), carcinogens such as diethylstilbestrol (Schiffmann and De Boni, 1991), and inherited genetic conditions such as Roberts syndrome (Jabs et al., 1991). Chromosomes, chromatids, and chromosome fragments that do not segregate properly often end up spatially separated from the bulk of the chromosomes and will reform a separate nuclear envelope after mitosis is completed. This results in a cell containing micronuclei. Sometimes these cells are described as multinucleate. Severe chromosome segregation defects will in turn inhibit cytokinesis giving rise to truly multinucleate cells (Schultz and Onfelt, 1994). The mechanism by which these diverse agents disrupt anaphase chromosome segregation is generally unclear. However, as more is known about the basic mechanisms of cell cycle regulation and chromosome segregation, certain lagging chromosome phenotypes can be mechanistically understood.

One mechanism by which lagging chromosomes can appear during anaphase is if a single chromatid establishes a connection to both spindle poles. This state has been induced experimentally by producing mono-centromeres either by separating sister chromatids with a laser (Khodjakov et al., 1997) or by preventing genome replication before mitosis (Wise and Brinkley, 1997). Such centromeres can congress to the metaphase plate but do not segregate well during anaphase because the single centromere has established connections with both spindle poles. Univalent chromosomes that do not establish a bipolar connection oscillate randomly from one pole to the other (Church and Lin, 1982). Bipolar attachment of a single chromatid, leading to lagging anaphase chromosomes, can also occur in dicentric chromosomes with two active centromeres (Haaf et al., 1992; Dawe and Cande, 1996; Fluminhan and Kameya, 1997). We believe that the lagging chromosomes seen in MCAK-depleted and GFP-motorless–transfected cells do not reflect this kind of defect because the chromosomes in our studies are monocentric, bivalent chromosomes. For a single centromere of a bivalent pair to establish a bipolar attachment, the entire centromere would have to twist perpendicular to the spindle axis as has been observed in meiotic cells (for review Nicklas, 1997). We do not see this occurring in GFP-motorless–containing fixed or live cells, therefore, we do not believe that MCAK is involved in error correction of monopolar attachment.

Another example of a well-characterized anaphase lagging chromosome phenotype is seen in zw10 mutants in *Drosophila melanogaster*. The lagging chromosomes which are seen in *Drosophila melanogaster* zw10 null mutants bear a striking resemblance to the MCAK phenotype (Williams et al., 1996). ZW10 is an 85-kD coiled-coil protein whose amino acid sequence does not contain any known functional domains. Like MCAK, zw10 null mutants exhibit a normal spindle profile for meiosis I and II (Williams et al., 1996). ZW10, however, colocalizes with CENP-E and dynein in, presumably, the outer corona of the kinetochore (Starr et al., 1997) and is involved in recruiting dynein/dynactin to the centromere (Starr et al., 1998). These data suggest that the ZW10-associated machinery is distinct from that of MCAK. The striking distribution of ZW10 along kinetochore microtubules at metaphase and the return to the centromere at anaphase suggests that ZW10 may be part of the tension-sensing checkpoint (Nicklas et al., 1995; Li and Nicklas, 1997) for the onset of anaphase (Williams et al., 1996). In our studies, live imaging indicates that the onset of chromosome separation is delayed in cells containing GFP-motorless MCAK. This may be significant in light of the observation by Faulkner et al. (1998) that MCAK is found on both active and inactive centromeres of dicentric chromosomes before sister chromatic arm separation. After sister chromatid arm separation, MCAK localized solely to the active centromere. The remarkable similarity between the zw10 mutant phenotype and that of GFP-motorless MCAK transfectants suggests that MCAK may also participate in the transition to anaphase but in a completely different fashion than ZW10 protein.

If MCAK plays a mechanical role in chromosome movement then what is the nature of MCAK activity? A variety of activities have been described for kinesins that are structurally related to MCAK. Kif2, a vesicle-associated motor, exhibits plus-end–directed motility (Noda et al., 1995), anterograde vesicle transport activity (Morfini et al., 1997) and microtubule cross-linking activity (Noda et al., 1995). MCAK also exhibits cross-linking activity in vitro (Coy, D., J. Howard, and L. Wordeman, unpublished observations). XKCM1, which is likely to be the *Xenopus* homologue of MCAK, promotes microtubule depolymerization (Walczak et al., 1996). While we cannot reconcile plus-end–directed motor activity with a role in centromere-dependent anaphase chromosome movement, both depolymerization and microtubule cross-linking are useful activities to have associated with anaphase kinetochores. In CHO cells, overexpression of MCAK leads to microtubule bundling and eventual loss of microtubule polymer. Although bundling supports the participation of MCAK in kinetochore fiber maturation (McEwen et al., 1997), the loss of microtubule polymer supports the hypothesis that MCAK may have depolymerizing activity (Walczak et al., 1996). It is unlikely that cross-linking activity alone could give rise to an eventual loss of all microtubule polymer.

If MCAK confers microtubule depolymerizing activity on the kinetochore, why is this activity required primarily during anaphase? Presumably during prometaphase con-

gression of bipolar chromosomes, anti-poleward movement is coordinated with microtubule depolymerization at the sister kinetochore. However, we have found that MCAK may be dispensable during prometaphase. In mammalian cells there is a transient increase in kinetochore microtubule number (McEwen et al., 1997) and stability (Zhai et al., 1995) that occurs before the onset of anaphase. Perhaps this is the only mitotic stage during which the resistance of kinetochore microtubules to depolymerization is significant. Perhaps during other stages of mitosis microtubules respond to mechanical compression on the microtubule ends and depolymerize accordingly. Congression, in this case, would be achieved by a combination of CENP-E activity (Schaar et al., 1997; Wood et al., 1997) and astral ejection forces (Ault et al., 1991) and without MCAK participation. Interestingly, in *S. cerevisiae* prometaphase oscillations of the same absolute amplitude as those seen in mammalian cells have been observed (Skibbens et al., 1995; Straight et al., 1997). These oscillations occur in the absence of MCAK as no obvious MCAK-related protein has been identified in the *S. cerevisiae* genome. Chromosome-to-pole movement has also been observed in *S. cerevisiae* presumably in conjunction with microtubule depolymerization at the kinetochore because the initial rates are more rapid than spindle elongation (Straight et al., 1997). Two distinct differences exist between centromere-dependent events in mammalian cells and those in yeast: mammalian kinetochores have (*a*) multi-microtubular kinetochores, and they (*b*) establish a metaphase plate. Other aspects of prometaphase and anaphase chromosome movement are surprisingly similar between *S. cerevisiae* and mammalian cells (Straight et al., 1997). CENP-E, which is also not present in *S. cerevisiae*, has been shown to be required for metaphase alignment (Schaar et al., 1997; Wood et al., 1997). Hence, it may be that MCAK is required for the transition from the metastable metaphase plate alignment, to poleward movement at the onset of anaphase. In *S. cerevisiae* sister chromosomes separate at anaphase onset regardless of their position within the spindle (Straight et al., 1997). Mammalian cells have obviously developed a more elaborate mechanism to coordinate poleward chromosome movement both temporally and spatially. This may reflect the greater contribution that anaphase A makes to anaphase chromosome segregation in mammalian cells relative to yeast. In *S. cerevisiae* the bulk of the absolute distance sister chromosomes travel to safely segregate is contributed by spindle elongation (anaphase B). In animal cells however, anaphase A makes a proportionally greater contribution to chromosome segregation. Any delay or lack of coordination in the onset and speed of anaphase chromosome segregation may be more likely to result in nondisjunction in animal cells where the distance chromosomes must travel during anaphase A is greater. Therefore, there may be a specialized requirement for MCAK-associated microtubule destabilization to coordinate the transition to anaphase chromosome movement in the presence of multi-microtubular, ultra-stable, mammalian kinetochore fibers.

Presently, our evidence does not fully support the model that MCAK is involved in modulating global microtubule dynamics within the cell or in spindle assembly, as has been demonstrated for XKCM1 (Walczak et al., 1996). Antisense-induced depletion of MCAK from mitotic or interphase cells does not appear to have an effect on microtubules in fixed interphase or mitotic cells. This could reflect differences between spindle assembly pathways mitotic versus meiotic systems or it could reflect technical constraints inherent in in vivo versus in vitro extracts. It may be that the minimum time requirement (24 h) for MCAK turnover in antisense-loaded cells triggers a modulation of the tubulin turnover dynamics that compensates for MCAK depletion. Nevertheless, the existence of such a compensatory response suggests that microtubule polymer levels are maintained at specific levels within the cell in spite of MCAK rather than using MCAK as an effector. Instead, the most immediate MCAK defect that is apparent in depleted and mutant cells is that of a chromosome segregation defect. Nevertheless, our MCAK overexpression phenotype supports the hypothesis that excess MCAK can diminish microtubule polymer in mitotic cells. We have also seen a similar defect in interphase cells (data not shown). Therefore, it seems likely that high concentrations of MCAK protein, such as is seen on the centromere, may be used during the metaphase-to-anaphase transition for destabilizing microtubules (Walczak et al., 1996) rather than plus-end–directed gliding motility (Noda et al., 1995). Whether microtubule cross-linking (Noda et al., 1995) is also a legitimate MCAK activity remains to be seen.

Interestingly, an MCAK-related protein, DSK1, isolated from the diatom *Cylindrotheca fusiformis* has been localized to the spindle midzone and implicated in anaphase B spindle elongation (Wein et al., 1996). Presumably, this function requires plus-end directed gliding motility as DSK1 appears to be anchored to a spindle midzone matrix in addition to microtubules. Significantly, an mAb produced against MCAK will inhibit spindle elongation in reactivated diatom spindles, as will antibodies produced against DSK1 (Wein et al., 1996). In our studies, we see an accumulation of both endogenous MCAK, GFP-MCAK, and GFP-motorless on spindle midzone microtubules during anaphase. Furthermore, we have seem some GFP-motorless live cells that appear to have impaired spindle elongation (Hunter, A.W., T. Maney, and L. Wordeman, unpublished results). Presently, we do not have a statistically significant number of cells that display this defect. This unpublished observation suggests that we may have failed to fully inhibit all MCAK-dependent functions in our transfected cells. Alternatively, if MCAK participates in the same process as ZW10 does, then it is not surprising that we see some but not all chromosomes lagging during anaphase. Zw10 null mutants display the same phenotype. However, functional redundancy is also a plausible explanation for our failure to inhibit the segregation of all chromosomes. Microtubule depolymerization alone has been shown to provide sufficient force to transport chromosomes poleward in the absence of ATP (Coue et al., 1991). Furthermore, other motors at the kinetochore, such as CENP-E, may facilitate poleward movement (Lombillo et al., 1995; Brown et al., 1996). In these cases, completely different sets of machinery may exhibit functional redundancy for anaphase chromosome movement. A final possibility is that we have failed to saturate all the potential MCAK binding sites. This could explain why we do not

see a full complement of lagging chromosomes. Also, because GFP-motorless accumulates in the nucleus before the onset of mitosis, the saturation of centromere binding sites may occur with greater efficiency than the saturation of spindle midzone binding sites that takes place during anaphase. Hence, it is possible that we have preferentially inhibited anaphase A (including the transition to anaphase) over anaphase B. Conversely, the possible involvement of DSK1 in anaphase A cannot be studied in the diatom for technical reasons. We are presently working on microinjection experiments that will help address the question of the potency of our mutant phenotype.

Motorless MCAK protein localizes to mitotic centromeres and interphase centrosomes, mitotic spindle poles and midbodies. Presumably this targeting occurs independently of microtubules because the motor domain of MCAK is required for microtubule binding in our assays. Microtubule-independent targeting has also been shown for the yeast kinesin–related protein Smy1 (Lillie and Brown, 1998). Microtubule-independent targeting to centromeres and centrosomes of motorless protein presumably involves other molecules that may be present in amounts below the level of detection of our immunoprecipitation assays. Furthermore, the bulk of MCAK in interphase cells is not targeted to specific subcellular structures. We are presently using the yeast two-hybrid system to identify molecules involved in targeting of MCAK to subcellular structures. The data we have presented here support the conclusion that MCAK may have novel motility properties such as bundling or depolymerizing activity that are important for anaphase chromosome segregation.

We are indebted to K. Allen (Cell Analysis Facility, Department of Immunology, University of Washington, Seattle, WA) for assistance with FACS® cell sorting. We gratefully acknowledge A. Bradshaw for help with the baculovirus-based expression system and gifts of Sf9 cells; S. Carlson for assistance with the gel exclusion chromatography and the sucrose gradients; D. Coy, W. Hancock, and J. Howard for assistance with the hydrodynamic calculations and for many helpful discussions. We thank L. Ginkel for many discussions and comments on the manuscript. Finally, the assistance of P. Brunner (W.M. Keck Center for Neural Imaging) has been indispensable for confocal and live cell imaging.

This study was supported by the Council for Tobacco Research and by GM53654A from the National Institutes of Health. T. Maney is supported by PHS-NRSA T326M07270.

Received for publication 24 March 1998 and in revised form 25 June 1998.

References

Ault, J.G., A.J. DeMarco, E.D. Salmon, and C.L. Rieder. 1991. Studies on the ejection properties of asters: astral microtubule turnover influences the oscillatory behavior and positioning of mono-oriented chromosomes. *J. Cell Sci.* 99:701–710.

Berger, B., D.B. Wilson, E. Wolf, T. Tonchev, M. Milla, and P.S. Kim. 1995. Predicting coiled coils by use of pairwise residue correlations. *Proc. Natl. Acad. Sci. USA*. 92:8259–8263.

Bloom, K. 1993. The centromere frontier: Kinetochore components, microtubule-based motility, and the CEN-value paradox. *Cell.* 73:621–624.

Brinkely, B.R., and J. Cartwright. 1971. Ultrastructural analysis of mitotic spindle elongation in mammalian cells in vitro: Direct microtubule counts. *J. Cell Biol.* 50:416–431.

Brown, K.D., K.W. Wood, and D.W. Cleveland. 1996. The kinesin-like protein CENP-E is kinetochore-associated throughout poleward chromosome segregation during anaphase-A. *J. Cell Sci.* 109:961–969.

Buhner, M., and H. Sund. 1969. Yeast alcohol dehydrogenase: -SH groups, disulfide groups, quaternary structure, and reactivation by reductive cleavage of disulfide groups. *Eur. J. Biochem.* 11:73–79.

Chalfie, M., Y. Tu, G. Euskirchen, W.W. Ward, and D.C. Prascher. 1994. Green fluorescent protein as a reporter for gene expression. *Science*. 263:802–805.

Church, K., and H.P. Lin. 1982. Meiosis in *Drosophila melanogaster*. II. The prometaphase-I kinetochore microtubule bundle and kinetochore orientation in males. *J. Cell Biol.* 93:365–373.

Coue, M., V.A. Lombillo, and J.R. McIntosh. 1991. Microtubule depolymerization promotes particle and chromosome movement in vitro. *J. Cell Biol.* 112: 1165–1175.

Dawe, R.K., and W.Z. Cande. 1996. Induction of centromeric activity in maize by suppressor of meiotic drive 1. *Proc. Natl. Acad. Sci. USA*. 93:8512–8517.

de Haen, C. 1987. Molecular weight standards for calibration of gel filtration and sodium dodecyl sulfate-Polyacrylamide gel electrophoresis: ferritin and apoferritin. *Anal. Biochem.* 166:235–245.

Deaven, L.L., and D.F. Petersen. 1973. The chromosomes of CHO, an aneuploid Chinese hamster cell line: G-band, C-band, and autoradiographic analysis. *Chromosoma (Berlin)*. 41:129–144.

Echeverri, C.J., B.M. Paschal, K.T. Vaughan, and R.B. Vallee. 1996. Molecular characterization of the 50-kD subunit of dynactin reveals function for the complex in chromosome alignment and spindle organization during mitosis. *J. Cell Biol.* 132:617–633.

Faulkner, N.E., B. Vig, C. Echeverri, L. Wordeman, and R.B. Vallee. 1998. Localization of motor-related proteins and associated complexes to active but not inactive, centromeres. *Hum. Mol. Genet.* 7:671–677.

Fluminhan, A., and T. Kameya. 1997. Involvement of knob heterochromatin in mitotic abnormalities in germinating aged seeds of maize. *Genome.* 40:91–98.

Haaf, T., P.E. Warburton, and H.F. Willard. 1992. Integration of human a-satellite DNA into simian chromosomes: centromere protein binding and disruption of normal chromosome segregation. *Cell.* 70:681–696.

Hagag, N., L. Diamond, R. Palermo, and S. Lyubsky. 1990. High expression of ras p21 correlates with increased rate of abnormal mitosis in NIH3T3 cells. *Oncogene.* 5:1481–1489.

Hesterberg, T.W., and J.C. Barrett. 1985. Induction by asbestos fibers of anaphase abnormalities: mechanism of aneuploidy induction and possibly carcinogenesis. *Carcinogenesis.* 6:473–475.

Horiike, K., H. Tojo, T. Yamano, and M. Nzaki. 1983. Interpretation of the stokes radius of macromolecules determined by gel filtration chromatography. *J. Biochem.* 93:99–106.

Hoyt, M.A., and J.R. Geiser. 1996. Genetic analysis of the mitotic spindle. *Annu. Rev. Genet.* 30:7–33.

Inou'e, S. 1997. The role of microtubule assembly dynamics in mitotic force generation and functional organization of living cells. *J. Struct. Biol.* 118:87–93.

Jabs, E.W., C.M. Tuck-Muller, R. Cusano, and J.B. Rattner. 1991. Studies of mitotic and centromere abnormalities in Roberts syndrome: implications for a defect in the mitotic mechanism. *Chromosoma (Berlin).* 100:251–261.

Karsenti, E., and A.A. Hyman. 1996. Morphogenetic properties of microtubules and mitotic spindle assembly. *Cell*. 84:401–410.

Khodjakov, A., R.W. Cole, B.F. McEwen, K.F. Buttle, and C.L. Rieder. 1997. Chromosome fragments possessing only one kinetochore can congress to the spindle equator. *J. Cell Biol.* 136:229–40.

Li, X., and R.B. Nicklas. 1997. Tension-sensitive kinetochore phosphorylation and the chromosome distribution checkpoint in praying mantis spermatocytes. *J. Cell Sci.* 110:537–545.

Lillie, S.H., and S.S. Brown. 1998. Smy1p, a kinesin-related protein that does not require microtubules. *J. Cell Biol.* 140:873–884.

Lombillo, V.A., C. Nislow, T.J. Yen, V.I. Gelfand, and J.R. McIntosh. 1995. Antibodies to the kinesin motor domain and CENP-E inhibit microtubule depolymerization-dependent motion of chromosomes in vitro. *J. Cell Biol.* 128:107–115.

Lupas, A., M. Van Dyke, and J. Stock. 1991. Predicting coiled-coils from protein sequences. *Science.* 252:1162–1164.

McEwen, B.F., A.B. Heagle, G.O. Cassels, K.F. Buttle, and C.L. Rieder. 1997. Kinetochore maturation of chromosome congression and anaphase onset. *J. Cell Biol.* 137:1567–1580.

Meluh, P., and D. Koshland. 1995. Evidence that the MIF2 gene of *Saccharomyces cerevisiae* encodes a centromere protein with homology to the mammalian centromere protein CENP-C. *Mol. Biol. Cell.* 6:793–807.

Merdes, A., K. Ramyar, J.D. Vechio, and D.W. Cleveland. 1996. A complex of NuMA and cytoplasmic dynein is essential for mitotic spindle assembly. *Cell*. 87:447–458.

Mitchison, T.J. 1989. Polewards microtubule flux in the mitotic spindle: Evidence from photoactivation of fluorescence. *J. Cell Biol.* 109:637–652.

Mitchison, T.J., L. Evans, E. Schulze, and M. Kirschner. 1986. Sites of microtubule assembly and disassembly in the mitotic spindle. *Cell.* 45:515–527.

Morfini, G., S. Quiroga, A. Rosa, K. Kosik, and A. Caceres. 1997. Suppression of KIF2 in PC12 cells alters the distribution of a growth cone nonsynaptic membrane receptor and inhibits neurite extension. *J. Cell Biol.* 138:657–669.

Nicklas, R.B. 1997. How cells get the right chromosomes. *Science*. 275:632–637.

Nicklas, R.B., S.C. Ward, and G.J. Gorbsky. 1995. Kinetochore chemistry is sensitive to tension and may link mitotic forces to a cell cycle checkpoint. *J. Cell Biol.* 130:929–939.

Noda, Y., R. Sato-Yoshitake, S. Kondo, M. Nangaku, and N. Hirokawa. 1995. KIF2 is a new microtubule-based anterograde motor that transports membranous organelles distinct from those carried by kinesin heavy chain or KIF3A/B. *J. Cell Biol.* 129:157–167.

Rieder, C.L., and E.D. Salmon. 1994. Motile kinetochores and polar ejection forces dictate chromosome position on the vertebrate mitotic spindle. *J. Cell Biol.* 124:223–233.

Sawin, K.E., and T.J. Mitchison. 1991. Poleward microtubule flux mitotic spindles assembled in vitro. *J. Cell Biol.* 112:941–954.

Schaar, B.T., G.K.T. Chan, P. Maddox, E.D. Salmon, and T.J. Yen. 1997. CENP-E function at kinetochores is essential for chromosome alignment. *J. Cell Biol.* 139:1373–1382.

Schiffmann, D., and U. De Boni. 1991. Dislocation of chromatin elements in prophase induced by diethylstilbestrol: a novel mechanism by which micronuclei can arise. *Mutat. Res.* 246:113–122.

Schultz, N., and A. Onfelt. 1994. Video time-lapse study of mitosis in binucleate V79 cells: chromosome segregation and cleavage. *Mutagenesis.* 9:117–123.

Skibbens, R.V., V.P. Skeen, and E.D. Salmon. 1993. Directional instability of kinetochore motility during chromosome congression and segregation in mitotic newt lung cells: A push-pull mechanism. *J. Cell Biol.* 122:859–875.

Starr, D.A., B.C. Williams, Z.X. Li, B. Etemad-Moghadam, R.K. Dawe, and M.L. Goldberg. 1997. Conservation of the centromere/kinetochore protein ZW10. *J. Cell Biol.* 138:1289–1301.

Starr, D.A., B.C. Williams, T.S. Hays, and M.L. Goldberg. 1998. ZW10 helps recruit dynactin and dynein to the kinetochore. *J. Cell Biol.* 142:763–774.

Straight, A.F., W.F. Marshall, J.W. Sedat, and A.W. Murray. 1997. Mitosis in living budding yeast: anaphase A but no metaphase plate. *Science.* 277:574–578.

Wadsworth, P., and E.D. Salmon. 1986. Analysis of the treadmilling model during metaphase of mitosis using fluorescence recovery after photobleaching. *J. Cell Biol.* 102:1032–1038.

Walczak, C.E., T.J. Mitchison, and A. Desai. 1996. XKCM1: a Xenopus kinesin-related protein that regulates microtubule dynamics during mitotic spindle assembly. *Cell.* 84:37–47.

Wein, H., M. Foss, B. Brady, and W.Z. Cande. 1996. DSK1, a novel kinesin-related protein from the diatom Cylindrotheca fusiformis that is involved in anaphase spindle elongation. *J. Cell Biol.* 133:595–604.

Winey, M., C.L. Mamay, E.T. O'Toole, D.N. Mastronarde, T.H. Giddings, Jr., K.L. McDonald, and J.R. McIntosh. 1995. Three-dimensional ultrastructural analysis of the *Saccharomyces cerevisiae* mitotic spindle. *J. Cell Biol.* 129: 1601–1615.

Williams, B.C., M. Gatti, and M.L. Goldberg. 1996. Bipolar spindle attachments affect redistributions of ZW10, a *Drosophila* centromere/kinetochore component required for accurate chromosome segregation. *J. Cell Biol.* 134: 1127–1140.

Wise, D.A., and B.R. Brinkley. 1997. Mitosis in cells with unreplicated genomes (MUGs): spindle assembly and behavior of centromere fragments. *Cell. Motil. Cytoskeleton.* 36:291–302.

Wood, K.W., R. Sakowicz, L.S.B. Goldstein, and D.W. Cleveland. 1997. CENP-E is a plus end-directed kinetochore motor required for metaphase chromosome alignment. *Cell.* 91:357–366.

Wordeman, L., and T.J. Mitchison. 1995. Identification and partial characterization of mitotic centromere-associated kinesin, a kinesin-related protein that associates with centromeres during mitosis. *J. Cell Biol.* 128:95–105.

Yen, T.J., G. Li, B.T. Schaar, I. Szilak, and D.W. Cleveland. 1992. CENP-E is a putative kinetochore motor that accumulates just before mitosis. *Nature.* 359:536–539.

Zhai, Y., P.J. Kronebusch, and G.G. Borisy. 1995. Kinetochore microtubule dynamics and the metaphase-anaphase transition. *J. Cell Biol.* 131:721–734.